The Effect of Radio Frequency Plasma Nitriding on Biocompatibility of Nickel-Titanium Shape Memory Alloys

Fayez Mahamoud El-Hossary[1], Sayed Mohammed Khalil[*2], Magdy Abdel Wahab Kassem[3], Medhat Abd EL Lateef[4], Doha Saber Mohamed[5], Khaled Lotfy[6]

[1,4,6]Physics Department, Faculty of Science, Sohag University, Sohag, Egypt

[2]Umm Al-Qura University, University Coolege, Qunfadah Center for Scientific Research (QCSR), Alqunfadah, KSA

[3]Department of Materials and Metallurgical Engineering, Faculty of Petroleum and Mining Engineering, Suez Canal University, Suez, Egypt

[5]Department of Histology, Faculty of Medicine, Sohag University, Sohag, Egypt

*[2]khalil_20002000@yahoo.com

***Abstract*- Nickel-titanium (Ni-Ti) shape memory alloys (SMAs) are attractive materials for orthopedic and dental implants, due to its two intrinsic properties including shape memory effect (SME) and superelasticity (SE), which may not be found in other commonly-used surgical metals. Possible Ni ion release, however, hampers their medical applications, particularly in orthopedic implants where fretting is always expected at the articulating surface. Inductively coupled radio frequency plasma (ICRFP) was employed to alter the surface of equiatomic Ni-Ti discs in order to create a barrier to out-diffusion of Ni ions from the bulk material. The ICRFP experiments were carried out with nitrogen, which promoted the formation of a titanium nitride layer on the surface of the Ni-Ti samples. The present paper explores the biocompatibility and performance of the ICRFP treated and untreated Ni-Ti samples. The results confirm that nitrogen plasma modified Ni-Ti alloys are potentially suitable materials for orthopedics without inducing harmful biological effects.**

Keywords- Nickel-Titanium (Ni-Ti); Superelasticity (SE); Shape Memory Effect (SME); Inductively Coupled Radio Frequency Plasma (ICRFP); Biocompatibility; Corrosion Resistance

I. INTRODUCTION

Nickel-titanium (Nitinol) shape memory alloys are attractive materials for orthopedic and dental implants due to their distinctive shape memory effect and superelasticity properties that may not be found in Ti alloys and stainless steels [1, 2]. However, adverse effects such as unfavorable osteogenesis process and osteonectin synthesis activity [3] as well as high cell death rate [4] have been reported for Ni-Ti alloys in spite of positive reports on its biocompatibility [5, 6]. This problem is suspected to stem from the release of toxic Ni ions due to the poor corrosion resistance of the materials in vitro and in vivo, consequently causing cytotoxicity and strong allergic reactions in patients [7]. Tantalum and oxygen have been implanted using plasma technology to improve the surface mechanical properties of these types of materials [8]. Furthermore, the use of nitrogen and oxygen plasma immersion ion implantation (PIII) can significantly improve the corrosion and wear properties of Ni-Ti due to the formation of TiN and TiO_2 layers, respectively, on the surface of the bulk material [9-12]. The aim of this work is to study the biocompatibility of Ni-Ti SMA for further safe use as a surgical implant material by investigating the formation of a nitrided layer produced by inductively coupled radio frequency plasma on the surface of equiatomic Ni-Ti samples.

II. EXPERIMENTAL METHODS

$Ni_{50}Ti_{50}$ SMAs have been fabricated by arc-melting [13]. For the present study, samples were prepared in the form of 2 mm thick sheet and cut into coupons of 10 mm × 20 mm. The specimens to be used as implants were cut to fit the size of the rabbit's femur, i.e., 1.2 mm in diameter and 15 mm in length.

A. Preparation Method of Alloys

The $Ni_{50}Ti_{50}$ alloys were prepared by arc-melting pure metals with nominal purities of 99.99 wt. % in an induction furnace under argon atmosphere (99.9999% purity). Produced castings were heated at 900 ℃ for 2 hours. The heated specimens were hot rolled with about 10% reduction each time at 800 ℃ up to 2 mm thickness [13].

B. Nitriding System

The nitriding treatment of Ni-Ti SMA samples was performed using a radio frequency (RF) inductively coupled glow discharge, with a continuous mode of operation at 13.56 MHz (525 W). Treatment duration was 10 min. Nitrogen (N_2) gas was

DOI: 10.5963/JBAP0501002

introduced to establish a gas pressure of 8-8.4 $\times 10^{-2}$ mbar, the distance between the sample holder surface and RF coil was 2.9 cm and the water cooling rate for samples was 1500 cm^3/min. The surface and cross-section morphology of tested samples with 2 mm thickness were examined using an optical microscope [13]. The crystallographic phases present in the surface region of the nitrided layer were studied by X-ray diffraction (XRD) using CuKα radiation in the Θ-2Θ geometry. The microhardness was measured by using a Wetzlar microhardness tester with the load of 0.98 N (100 g) [13, 14].

C. Corrosion Tests

Corrosion-resistance performance tests were carried out in the Ringer's solution 6.00 g/l NaCl, 3.20 g/l sodium lactate, 0.27 g/l $CaCl_2$, 0.4 g/l KCl. (pH=7.4) at a temperature of 37±1 ℃. The test solution was not used more than 2 times due to possible breakdown of solution purity. The sample was pressed into a holder with a Teflon gasket, which ensured that only the front part of the sample 0.78 cm^2 was in contact with the electrolyte. The electrochemical testing process was carried out without aeration. The experimental setup consisted of a conventional three-electrode cell containing the working electrode, reference electrode (Ag/AgCl) and platinum as the counter electrode. The potentiodynamic experiment was carried out using a computer-controlled potentiostat (Gill AC, model 88). Polarization experiments started after the specimen was immersed in the experimental solution for 1 hour under open circuit conditions and performed at a rate of 100 mV/min. The electrochemical behavior of the nitrided Ni-Ti samples was compared with that of untreated Ni-Ti samples. The electrochemical tests were conducted in Ringer's solution at a pH of 7.4 and temperature of 37±0.5 ^oC. The corrosion behaviour of tested specimens was studied by open circuit test potentiodynamic polarization, cyclic polarization, and chronoamperometric/current – time transient and impedance measurements. The electrochemical tests were conducted after immersed the samples in Ringer's solution for 10 h, 1 week, 2 weeks, 3 weeks and 4 weeks.

D. Surgical Procedures

New Zealand rabbits of either sex male, weighing 2-2.5 Kg, were raised at the center animal house of Assiut University and housed in individual cages in air-conditioned environment. The room was artificially illuminated on a schedule of 12 h of light and 12 h of darkness. They were allowed to acclimatize for 7 days before starting the study, and were provided free access to food and water throughout the study. Rabbits were divided into 3 groups of 6 New Zealand rabbits each. Group I was composed of rabbits implanted with untreated Ni-Ti samples while group II was composed of rabbits implanted with treated samples. The control group (group III) was also composed of 6 New Zealand rabbits but these animals have not been subjected to any implantation procedure. The animals were prepared by intramuscularly injecting Mepecaine (15 mg/kg). Under sterile surgical conditions, the femur was exposed through a medical incision. One slightly oversized hole (1.2 mm in diameter) were made in the later cortex bone of one of the rabbit's femurs using a low-speed dental burr under saline irrigation. The implants were randomly inserted in the holes with light pressure. The long axis of the cylinder was parallel to the long axis of the femur. The rabbits were sacrificed at 8 week post-operation. Before being killed, the rabbits took Teramycine (100 mg/kg/day) for 6 days as antibiotic.

E. Studies

1) Determination of the Rate of Metal Dissolution from Ni-Ti to Distant Organs

The concentrations of Ni in various organs were assessed 8 weeks after the implantation procedure, to find out whether there had been release or accumulation of ions. The samples were first freeze-dried for 7 days. After that, they were weighed accurately (approximately to 0.1g) in Teflon decomposition vessels. Five milliliters of ultra pure nitric acid were added. The samples were decomposed in a microwave oven and diluted in 10 ml of distilled water. Ni release was determined by graphite furnace atomic absorption spectrometry (Perkin-Elmer 2380) and the concentrations were given as dry weights.

2) Measurement of Blood Biochemical Variables

Arterial blood samples were collected in heparinized syringes. The following variables were measured by atomic biochemistry analyzers (Pritest ECO, ACO 450307RBK, India): urea, creatinine, aspartate aminotrasferase (AST) and alanine aminotransferase (ALT).

3) Histological Change

Small pieces of fresh liver and kidney were pre-fixed in 1:1 mixture of 2% paraformaldehyde and 2.5% glutraldhyde in phosphate buffer, post-fixed in 1% osmium tetroxide for 1 hour and washed in buffer solution. They were washed in 30% alcohol and dehydrated in graded series of ethanol. Specimens were embedded in epon after treatment in propylene oxide, and sectioned in ultra tome using glass knives. Semi thin sections were stained with toluidine blue and photographed with light microscope. Ultrathin sections were stained with urany l acetate for 5 minutes and lead citrate for 5 minutes. They were viewed under a Jeol 1010 TEM.

DOI: 10.5963/JBAP0501002

III. RESULT AND DISCUSSION

A. X-Ray Diffraction Analysis

The structural characteristics of the layers formed on Ni-Ti samples surface were investigated by XRD. Fig. 1(a) shows the diffraction peaks of an as-received (untreated) Ni-Ti sample. The highly intense peak at 45.1 º could be associated with the B19` martensite phase (a Ni-Ti phase) [15]. The diffractogram does not exhibit peaks related to the oxide phase observed on the surface. Diffraction peaks related to oxide phases could not be detected using the experimental setup available because they are too thin or not crystalline. This observation well agrees with Neelakantan et al. 2009 [15]. Fig. 1(b) shows the diffraction peaks of a Ni-Ti SMA sample treated at 525W. It can be seen that the XRD pattern is composed of TiN and Ti_2Ni phases. The formation of these phases could be due to the fact that Ti atoms react more easily with N than Ni [16]. No diffraction peaks attributable to B19` martensite (NiTi phase) were detected. In addition, peaks of a Ni-rich phase are not observed, most likely, because at 800 ℃ Ni atoms diffuse into the Ni-Ti matrix since both the diffusion rate and the saturated quantity of dissolved Ni atoms in the Ni-Ti matrix are high enough. On the other hand, peaks related to the NiN phase are not present. This could be due to the fact that the heat of formation of TiN is -305.6 kJ/mol [17] and that Ni nitrides such as Ni_3N are unstable compared to TiN [18]. Furthermore, the Ni_3Ti intermediate layer which would decrease the performance of the material cannot be detected using the available XRD setup [19].

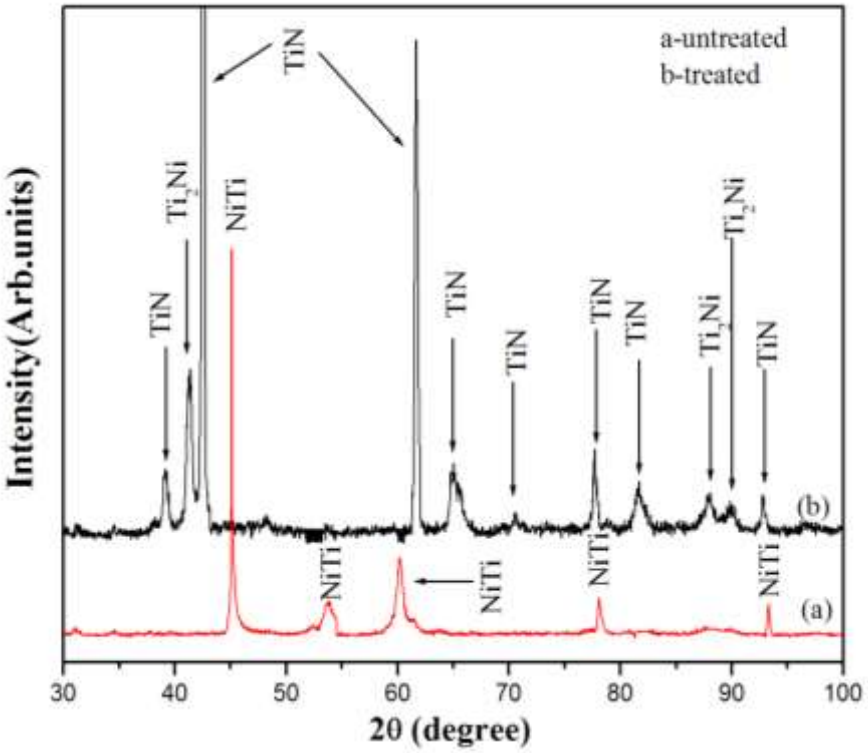

Fig.1 X-ray diffraction patterns for NiTi shape memory alloys (a) untreated; (b) treated by plasma processing power at 525 W

B. Electrochemical Characterization

The essential readings from our electrochemical tests in lieu of the complete potentiodynamic curves are shown in Table 1. The results reflected the high corrosion resistance for treated Ni-Ti samples when compared to the untreated samples. Moreover, it is known that nitrogen may be involved chemically in establishing the passive layer. If nitrogen becomes oxidized it may enhance the passivation in several ways [20]: (i) the oxidized nitrogen species can become an intimate chemical part of the bonding in the passivation layer by producing an oxide film of a lower ion conductivity [21]; (ii) it may act catalytically to produce a special chemical state of the oxide, such as a higher concentration of the stable Ti^{4+} ion. The resulting enhanced corrosion resistance is then due to the formation and maintenance of a more passive oxide layer. This enhanced production of Ti^{4+} with the nitrogen content in the combined layer is responsible for the improved corrosion passivation of plasma-nitrided Ni-Ti SMAs in Ringer's solution. Thus, the beneficial effect of nitrogen in improving the corrosion resistance of Ti nitride is mainly explained by the formation of a stable and insoluble oxide layer that has reduced ions diffusion. These results show that RF plasma nitriding is a promising method to improve the corrosion resistance of Ni-Ti SMAs in Ringer's solution. Therefore, the corrosion resistance of the 2 samples in descending order is nitrogen-treated Ni-Ti > untreated Ni-Ti. The nitrogen-treated samples exhibit higher breakdown potential than the untreated Ni-Ti samples.

DOI: 10.5963/JBAP0501002

TABLE 1 A SUMMARY OF ELECTROCHEMICAL PARAMETER FOR UNTREATED AND TREATED NI-TI WHICH OBTAINED FROM ELECTROCHEMICAL MEASUREMENTS

$I_{mm.}$ Time	I_{corr} $\times10^{-8}$ A		I_{dens} $\times10^{-7}$ A		LPR $\times10^{6}$ Ω.Cm^2		E_{corr} (V)		Corrosion rate $\times10^{-6}$ mm/year	
	Un.	treated	Un.	treated	Un.	treated	Un.	treated	Un.	treated
10 h.	0.88	2.3	1.7	8.2	3.6	110	-331	- 32	200	7
1 W.	2.2	2.8	19	10	1	90	-379	- 45	600	8.6
2 W.	10	9	100	30	0.2	30	-453	- 72	2800	25
3 W.	200	10	250	40	0.01	20	-564	- 99	57000	28
4 W.	400	70	770	50	0.007	4	-675	- 133	100000	200

C. Surface Morphology

Optical microscopy (OM) served to identify the changes on the surface of the untreated and treated Ni-Ti samples subject to corrosion measurements performed in Ringer's solution. Fig. 2(a, b) depict the changes observed after 1 week of experiments. In Fig. 2(a), numerous small pits over the entire surface are observed for untreated Ni-Ti sample which is in good agreement with the corrosion data. On the other hand, no corrosion pits can be detected on the surface of the treated sample exposed to simulated body fluid environmental conditions (fig. 2(b)). These observations support the results obtained from the corrosion measurements. Thus, equiatomic Ni-Ti SMAs with surfaces modified by the ICRFP technique with nitrogen is a promising material for biomedical applications [22].

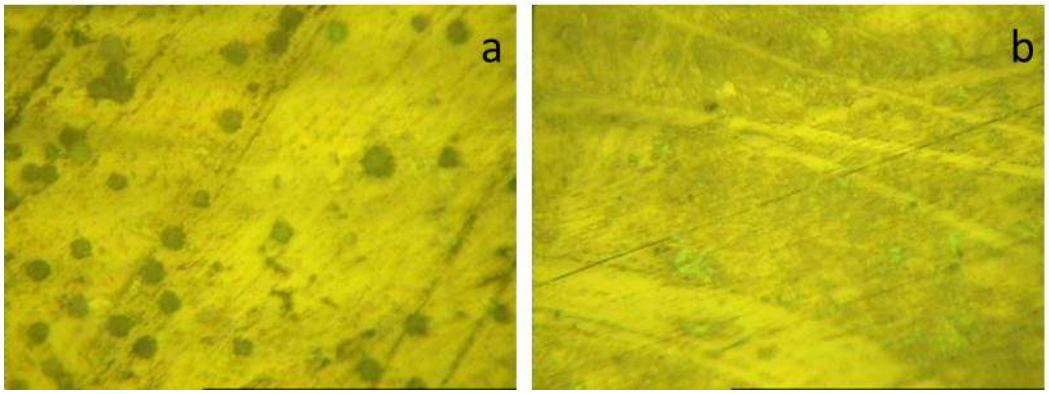

Fig. 2 Optical micrographs of the surface morphology of Ni-Ti shape memory alloy samples treated for plasma processing power at 525W (a) untreated (b) treated after corrosion measurements by immersed in Ringer's solution for one week

Fig. 3(a, b) show representative surface structures of untreated and RF plasma nitrided Ni-Ti samples after corrosion measurements by immersed in Ringer's solution for 4 weeks. The optical micrograph recorded for the untreated sample shows that many large pits are present on the surface of the sample as shown in Fig. 3a. These are much larger than the ones observed for the samples immersed in Ringer's solution for 1 week as shown in Fig. 2a. This result is attributed to a high release of Ni metal ions into the environment, which suggests that the dissolution of the passive film occurred and that local corrosion might have taken place by means of anion penetration [23]. On the other hand, for nitrided Ni-Ti samples no pits are found on the surface as shown in Fig. 3b. This result agrees with the obtained corrosion measurements which revealed a wide passivity range that extends up to very high potentials and absence of hysteresis loop; these features indicate high resistance to pitting [24].

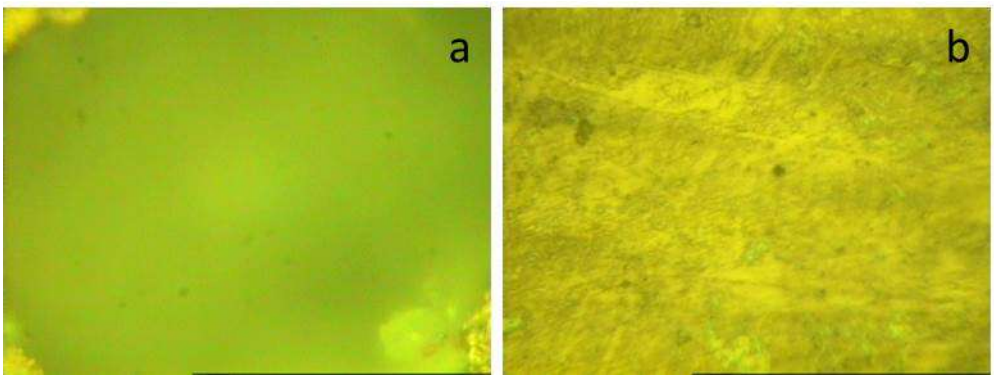

Fig. 3 Optical micrographs of the surface morphology of Ni-Ti shape memory alloy samples treated for plasma processing power at 525W (a) untreated; (b) treated after corrosion measurements by immersed in Ringer's solution for four weeks

DOI: 10.5963/JBAP0501002

D. Biocompatibility

In this section the effect of RF plasma nitriding on the biocompatibility of equiatomic Ni-Ti SMAs by implantation in rabbits was investigated. Figures 4 and 5 show radiographs recorded for rabbit's legs with implants post-operation, namely with untreated and treated implants. The radiographs show one slightly oversized hole in the right femur for the 2 rabbits. On the other hand, bone atrophic atrophy was observed in the case of the rabbits implanted with untreated Ni-Ti (Fig. 6) and RF plasma nitrided Ni-Ti samples (Fig. 7) after 8 weeks of operation. However, although a bone atrophic change was observed at the femur in both cases the change observed for the rabbit with the treated implant is lower than for the one with the untreated implant. Niinomi [25] has studied the mechanical biocompatibility of low rigidity Ti alloys for biomedical applications. The author reported that a little atrophic change was observed after 20 weeks at the posterior tibia bone of rabbits implanted with Ti–29Nb–13Ta–4.6Zr, while a little atrophic change was seemed to be observed at 18 weeks in the case of rabbits implanted with Ti–6Al–4V. Here, the radiograph recorded after 8 weeks of operation for the rabbits implanted with untreated NiTi samples shows traces of the hole that has been open in the bone, which indicates incomplete bone healing as shown in Fig. 8. In the case of the rabbits implanted with Ni-Ti samples modified by RF plasma nitriding no traces of the holes could be observed as shown in Fig. 9. Therefore, it is possible to conclude that the RF plasma nitriding technique created a surface layer on the Ni-Ti samples that promotes bone healing. Piscanec et al. [26] have reported that the surface of nitrogen treated Ni-Ti samples comprise a mixture of TiO_x and TiN. Furthermore, they mentioned the formation of TiO_xN_y oxynitride on the Ti surface after nitriding. This specific compound is believed to favor the formation of bone-like materials under in vivo conditions.

Fig. 4 Radiograph of untreated Ni-Ti shape memory alloy implant in rabbits post-operation (the arrow refer to the hole)

DOI: 10.5963/JBAP0501002

Fig. 5 Radiograph of treated Ni-Ti shape memory alloy implant in rabbits post-operation (the arrow refer to the hole)

DOI: 10.5963/JBAP0501002

Fig. 6 Radiograph of untreated Ni-Ti shape memory alloy implant in rabbits after 8 weeks from operation

DOI: 10.5963/JBAP0501002

Fig. 7 Radiograph of treated Ni-Ti shape memory alloy implant in rabbits after 8 weeks from operation

DOI: 10.5963/JBAP0501002

Fig. 8 Radiograph of untreated Ni-Ti shape memory alloy implant in rabbits after 8 weeks from operation (the arrow refer to the hole)

DOI: 10.5963/JBAP0501002

Fig. 9 Radiograph of treated Ni-Ti shape memory alloy implant in rabbits after 8 weeks from operation

The concentrations of Ni in kidney and liver were assessed after implantation of untreated and treated Ni-Ti samples in rabbit's tibia at 8 weeks. Data obtained using the graphite furnace atomic absorption spectroscopy (GFAAS) technique is summarized in Table 2. It has been found that for the rabbits implanted with untreated samples for 8 weeks the highest Ni levels were detected in the kidney (477.5 ± 9.1 μg/g dry weight). In the case of the group with treated Ni-Ti implants the higher Ni levels were also observed in the kidney but the values were 43 ± 5.2 μg/g dry weight. It should be point out that in the case of control group the Ni levels detected in the kidney were 14.5 ± 1.8 μg/g dry weight. Thus, the experiments show that after 8 weeks of implantation, the Ni concentration in the kidneys of the rabbits increased 2.9 fold in the case of rabbits with treated samples and 32.9 fold in the case of rabbits with untreated samples.

The Ni concentration values detected in the liver for the control group, the group with untreated implants and the group with treated implants were 25.5 ± 5.31, 151 ± 5.34 and 33 ± 4.6 μg/g dry weight, respectively. Thus, after 8 weeks, Ni concentration increased 1.3 fold in the liver of rabbits with treated samples and 6 fold for the group implanted with untreated Ni-Ti samples. Therefore, there was a significant increase ($P < 0.05$) of Ni levels in kidney and liver in the case of the untreated groups but a significant lower increase ($P < 0.05$) in the case of the group with treated implants, with respect to control one. It can be concluded that the lower Ni release from nitrided Ni-Ti implants with respect to the untreated ones may be attributed to TiN produced by RF plasma nitriding, which improved the corrosion resistance and the biocompatibility of the Ni-Ti SMAs. Matsumoto et al. [27] have reported atomic absorption spectroscopic analyses concerning Ni release after implantation of Ni-Ti samples in rabbits. According to their observations, after 6 ~ 9 h, implantation Ni blood concentration had reached 28 ± 11 ppb. After 4 weeks, Ni concentration had increased 4 fold in the kidneys (140 ± 43 ppb), 2 fold in the liver (40 ± 18 ppb), and 10 fold in urine (90 ± 35 ppb). The mechanisms associated with Ni release in Ni-Ti SMAs are well documented as well as surface conditions and sterilization procedures to be employed. Ryhanen [28] using graphite furnace atomic absorption spectroscopy reported that there was no statistical difference between the Ni concentrations induced by Nitinol (mechanically polished, autoclaved for 30 min at 121 ℃) and stainless steel (electropolished, autoclaved) implants. The highest concentration after 26 weeks of implantation was observed in the kidneys (1.4 ± 1.0 μg/g, dry weight), and decreased by 60 weeks. On the other hand, it can be observed that, in the case of the spleen, the Ni ion concentration increases slightly from (0.17 ± 0.06 μg/g) for 26 weeks to (1.14 ± 1.1 μg/g) for 60 weeks. However, these 2 values are not significantly different given the experimental uncertainty. Also, Ryhanen [28] reported a significant increase of spleen iron content (from 6010 ± 1950 to 14200 ± 4370 μg/g) during the same time interval on exposure to stainless steel.

TABLE 2 THE CONCENTRATIONS OF NICKEL IN KIDNEY AND LIVER AFTER IMPLANTATION OF UNTREATED AND TREATED NI-TI SHAPE MEMORY ALLOYS IN RABBIT'S TIBIA AT 8 WEEKS

Organ	Control group (μg/g)	Untreated group (μg/g)	Treated group (μg/g)
Kidney	14.5±1.8	477.5±9.1	43±5.2
Liver	25.5±5.31	151.1±5.34	33±4.6

DOI: 10.5963/JBAP0501002

The data obtained from kidney function are summarized in Table 3. These results show that blood urea and serum creatinine for the control group and the group with nitrided Ni-Ti implants are 46.5 ± 3.2, 1.56 ± 0.6 mg/dl and 48.16 ± 3.8, 1.76 ± 0.28 mg/dl, respectively (reference range: 10.7 ~ 53.5 and 0.5 ~ 2.6 mg/dl) [29], which reveals a significant lower increase ($P < 0.05$) with respect to the control group. On the other hand, the values obtained for the untreated group indicate a significant increase in blood urea and serum creatinine, i.e. 63 ± 4.7, 3.05 ± 0.36 mg/dl respectively. Furthermore, the blood urea and serum creatinine values for group with treated Ni-Ti implants reveal a significant lower increase ($P < 0.05$) with respect to the control group but a significant increase ($P < 0.05$) in the case of the group with untreated Ni-Ti implants.

TABLE 3 KIDNEY ENZYMES FOR CONTROL, UNTREATED AND TREATED GROUPS

Test	Control	Untreated	Treated	Reference Range
Blood Urea (mg/dl)	46.5±3.2	63±4.7	48.16±3.8	10.7 -53.5
Serum Creatinine (mg/dl)	1.56±0.6	3.05±0.36	1.76±0.28	0.5 -2.6

The results obtained from liver enzymes are summarized in Table 4. The values for aspartate aminotrasferase (AST) and alanine aminotransferase (ALT) for the control group are 26.16 ± 4.35 and 43.5 ± 3.8 u/l, respectively, which are within the normal range (10 ~ 98 and 25 ~ 65 u/l) [27]. On the other hand, AST and ALT values for the group with nitrided Ni-Ti implants are 101.8 ± 3.5 and 76.16 ± 4.53 u/l, respectively, which reveals a significant lower increase ($P < 0.05$) with respect to the control group. However, a significant increase ($P < 0.05$) has been observed in the case of group of rabbits with untreated implants, i.e. 126.3 ± 5.2 and 207.66 ± 5.16 u/l (reference range: 10 ~ 98 and 25 ~ 65 u/l).

TABLE 4 LIVER ENZYMES FOR CONTROL, UNTREATED AND TREATED GROUPS

Test	Control	Untreated	Treated	Reference Range
AST (U/L)	26.16±4.35	126.3±5.2	101.8±3.5	10-98
ALT (U/L)	43.5±3.8	207.66±5.16	76.16±4.53	25-65

The results presented above allow us to conclude that the high increase of kidney and liver enzymes for the rabbits with untreated Ni-Ti implants can be attributed to the high Ni release from the Ni-Ti implant. On the other hand, the moderate kidney and liver enzymes observed for the group of rabbits with treated Ni-Ti implants can be attributed to TiN present on the surface of the sample, which has been produced by RF plasma nitriding. This topmost layer inhibits Ni release from the Ni-Ti SMAs and enhances the blood biocompatibility for this alloy.

E. Histological Changes

Fig. 10(a) depicts the histological liver change observed for a rabbit from the control group. From this figure it can be seen that the control liver cells appeared to be arranged in plates separated by blood sinusoids. Hepatocytes have granular cytoplasm and vesicular rounded nuclei. However in the group implanted with untreated Ni-Ti SMAs it has been observed a loss of cytoplasmic granules of hepatocytes. The cytoplasm appeared vacuolated. Some nuclei of hepatocytes appeared deeply stained. Moreover, dilated blood sinusoids were observed when compared to the control group as shown in Fig. 10(b). Fig. 10(c) depicts the histological change in the case of the group with treated Ni-Ti SMAs implants. This figure suggests that no relevant changes occurred in the liver apart from vacuolated cytoplasm of some hepatocytes.

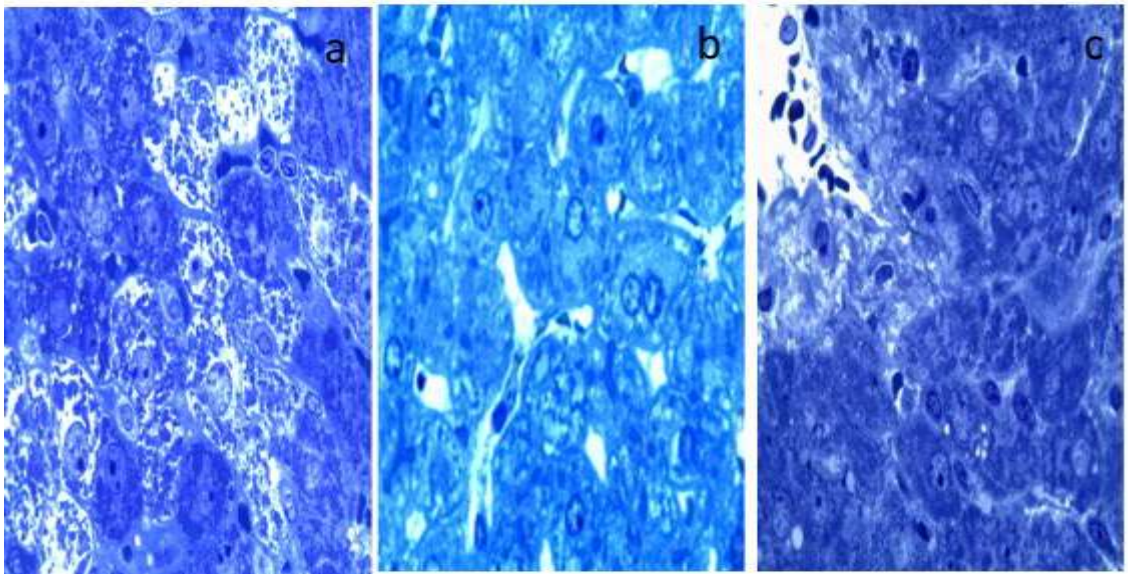

Fig. 10 Photomicrograph of (a) control liver; (b) untreated Ni-Ti shape memory alloy implant in rabbits; (c) treated Ni-Ti shape memory alloy implant in rabbits

DOI: 10.5963/JBAP0501002

Fig. 11(a) depicts the histological kidney change in the case of control rabbits. It can be observed that the renal corpuscle appears with its renal glomeruli, Bowman's capsule and mesangial cells. The proximal convoluted tubules (P.C.T) have cuboidal cells with apical brush border and vesicular rounded nuclei. The distal convoluted tubules (D.C.T) are formed of cuboidal cells with rounded vesicular nuclei. In the case of the group implanted with untreated Ni-Ti SMA, the renal glomeruli appears dilated and the cytoplasm of P.C.T vacuolated. Moreover, destruction of some P.C.T cells was observed, and their brush borders were lost. Dilatation of D.C.T cells was observed as can be seen in Fig. 11(b). Fig. 11(c) depicts the histological change in group implanted with treated Ni-Ti SMA implant. We can observe a dilatation of the renal glomeruli and that the cytoplasm of P.C.T was vacuolated and that the D.C.T is dilated.

Therefore, the high histological changes between the control rabbits and the group implanted with untreated Ni-Ti SMAs can be attributed to the high Ni release from untreated Ni-Ti samples. On the other hand, the moderate histological changes between the control rabbits group and the group implanted with treated Ni-Ti samples can be attributed to the low Ni release from treated Ni-Ti samples or the side effect of antibiotic which had been administered to rabbits after operation.

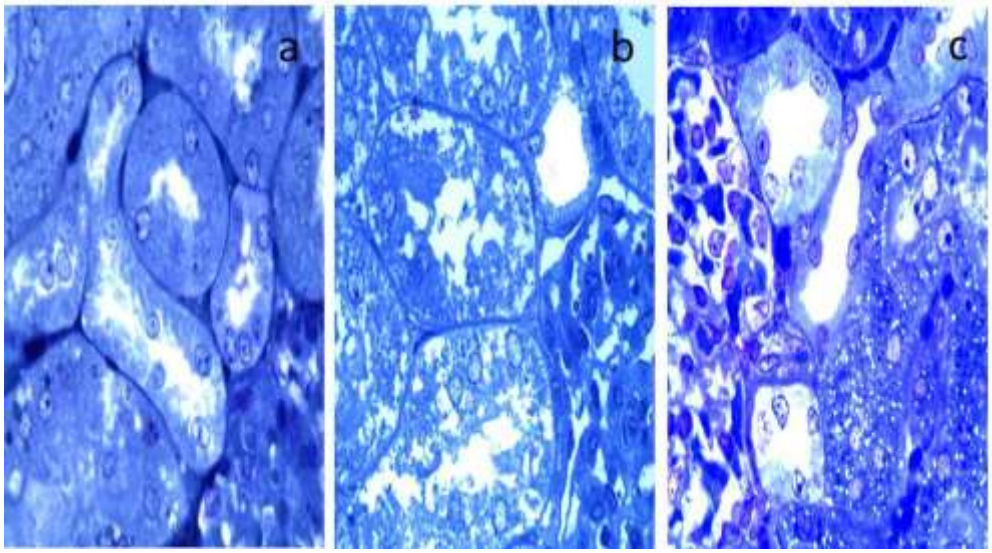

Fig. 11 Photomicrograph of (a) control kidney; (b) untreated Ni-Ti shape memory alloy implant in rabbits; (c) treated Ni-Ti shape memory alloy implant in rabbits

IV. CONCLUSION

Based on the obtained results, the following conclusions could be derived. Examination of structures revealed that the nitrided equiatomic Ni-Ti SMAs have excellent resistance to pitting and crevice corrosion. X-ray diffractions of nitrided NiTi SMAs showed the predominance of new phases TiN and Ti_2Ni phases and disappearance of the phase of B19` martensite (NiTi). The enhancement in the corrosion resistance of nitrided samples is due to the formation of TiN layer. Atomic absorption analyses demonstrated that the decrease of Ni release from nitrided Ni-Ti SMAs with respect to untreated one, can be attributed to TiN formed by RF plasma nitriding. TiN plays a crucial role in enhancement the blood biocompatibility of Ni-Ti SMAs since it serves as mask to inhibit Ni release. The moderate Kidney and Liver enzymes for rabbits implanted with treated Ni-Ti SMAs samples rely on TiN produced by RF plasma nitriding, which inhibit Ni release from the Ni-Ti SMAs. Generally, the obtained results indicate that RF plasma nitriding is a promising method to improve the biocompatibility of Ni-Ti SMAs.

REFERENCES

[1] M. F. Chen, X. J. Yang, R. X. Hu, Z. D. Cui, and H. C. Man, "Bioactive NiTi shape memory alloy used as bone bonding implants," *Mater. Sci. and Eng.*, vol. 24, pp. 497-502, 2004.

[2] J. Ryhanen, M. Kallioinen, W. Serlo, P. Peramaki, J. Junila, P. Sandvik, E. Niemela, and J. Tuukkanen, "Bone healing and mineralization, implant corrosion, and trace metals after nickel–titanium shape memory metal intramedullary fixation," *J. Biomed. Materi. Res.*, vol. 47, pp. 472-480, 1999.

[3] W. Jia, M. W. Beatty, R. A. Reinhardt, T. M. Petro, D. M. Cohen, C. R. Maze, E. A. Strom, and M. Hoffman, "Nickel release from orthodontic arch wires and cellular immune response to various nickel concentrations," *J. Biomed. Mater. Res.*, vol. 48, pp. 488-495, 1999.

[4] M. Es-Souni, M. Es-Souni, and H. F. Brandies, "On the properties of two binary NiTi shape memory alloys. Effects of surface finish on the corrosion behaviour and in vitro biocompatibility," *Biomaterials*, vol. 23, pp. 2887-2894, 2002.

[5] M. Es-Souni, M. Es-Souni, and H. F. Brandies, "On the transformation behaviour, mechanical properties and biocompatibility of two NiTi-based shape memory alloys: $NiTi_{42}$ and $NiTi_{42}Cu_7$," *Biomaterials*, vol. 22, pp. 2153-2161, 2001.

DOI: 10.5963/JBAP0501002

[6] D. Bogdanski, M. Koller, D. Muller, G. Muhr, M. Bram, H. P. Buchkremer, D. Stover, J. Choi, and M. Epple, "Easy assessment of the biocompatibility of Ni-Ti alloys by in vitro cell culture experiments on a functionally graded Ni-NiTi-Ti material," *Biomaterials*, vol. 23, pp. 4549-4555, 2002.

[7] C. C. Shih, S. J. Lin, Y. L. Chen, Y. Y. Su, S. T. Lai, G. J. Wu, C. F. Kwok, and K. H. Chung, "The cytotoxicity of corrosion products of nitinol stent wire on cultured smooth muscle cells," *J. Biomed. Mater. Res.*, vol. 52, pp. 395-403, 2000.

[8] L. Tan, R. A. Dodd, and W. C. Crone, "Corrosion and wear-corrosion behavior of NiTi modified by plasma source ion implantation," *Biomaterials*, vol. 24, pp. 3931-3939, 2003.

[9] R. W. Y. Poon, K. W. K. Yeung, X. Y. Liu, P. K. Chu, C. Y. Chung, W. W. Lu, K. M. C. Cheung, and D. Chan, "Carbon plasma immersion ion implantation of nickel-titanium shape memory alloy," *Biomaterials*, vol. 26, pp. 2265-2272, 2005.

[10] K. W. K. Yeung, R. W. Y. Poon, X. Y. Liu, J. P. Y. Ho, C. Y. Chung, P. K. Chu, W. W. Lu, D. Chan, and K. M. C. Cheung, "Investigation of nickel suppression and cytocompatibility of surface-treated nickel-titanium shape memory alloys by using plasma immersion ion implantation," *J. Biomed. Mater. Res. A*, vol. 72, pp. 238-245, 2005.

[11] R. W. Y Poon, X. Y. Liu, C. Y. Chung, P. K. Chu, K. W. K. Yeung, W. W. Lu, and K. M. C Cheung, "Surface and corrosion characteristics of carbon plasma implanted and deposited nickel-titanium alloy," *J. Vac. Sci. Technol. A*, vol. 23, pp. 525-530, 2005.

[12] K. W. K. Yeung, R. W. Y. Poon, X. Y. Liu, J. P. Y. Ho, C. Y. Chung, P. K. Chu, W. W. Lu, D. Chan, and K. M. C. Cheung, "Corrosion resistance, surface mechanical properties, and cytocompatibility of plasma immersion ion implantation-treated nickel-titanium shape memory alloys," *J. Biomed. Mater. Res. A*, vol. 75, pp. 256-267, 2005.

[13] F. M. El-Hossary, S. M. Khalil, M. A. W. Kassem, M. A. E. Lateef, and K. Lotfy, "Tribological Properties of Biomedical NiTi Shape Memory Alloy after Rf Plasma Nitriding," *Journal of Basic and Applied Physics*, vol. 3, pp. 54-67, 2014

[14] H. C. Man, and N. Q. Zhao, "Phase transformation characteristics of laser gas nitrided NiTi shape memory alloy," Surf. Coat. Technol., vol. 200, pp. 5598-5605, 2006.

[15] S. K. Wu, H. C. Lin, and C. Y. Lee, "Gas nitriding of an equiatomic TiNi shape-memory alloy: Part I: Nitriding parameters and microstructure characterization," *Surf. Coat. Technol.*, vol. 113, pp. 17-24, 1999.

[16] L. Neelakantan, S. Swaminathan, M. Spiegel, G. Eggeler, and A. Hassel, "Selective surface oxidation and nitridation of NiTi shape memory alloys by reduction annealing, corrosion science," *Corrosion Science*, vol. 51, pp. 635-641, 2009.

[17] R. Mientus, and K. Ellmer, "Reactive DC magnetron sputtering of elemental targets in Ar/N_2 mixtures: relation between the discharge characteristics and the heat of formation of the corresponding nitrides," *Surf. Coat. Technol.*, vol. 1093, pp. 116-119, 1999.

[18] K. Yokota, K. Nakamura, T. Kasuya, S. Tamura, T. Sugimoto, K. Akamatsu, K. Nakao, and F. Miyashita, "Compositional structure of dual TiNO layers deposited on SUS 304 by an IBAD technique," *Surf. Coat. Technol.*, vol. 568, pp. 158-159, 2002.

[19] J. Lelatkoa, T. Goryczka, T. Wierzchon, M. Ossowski, B. Losiewicz, E. Rowinski, and H. Morawiec, "Surface modification of Ni-Ti alloy by low-temperature nitriding Process," pp. 1-6, 2009, DOI:10.1051/esomat/20090502.

[20] D. Cocke, M. Rajmanand, and S. Vepreck, "The surface properties and reactivities of plasma nitrided iron and their relation to corrosion passivation electrochemical science and technology," *J. Electrochem. Soc.*, vol. 136, p. 3655, 1989.

[21] A. Akolzin, Y. Kharitonov, and S. Kovalenko, "In Enhanced corrosion resistance properties of radiofrequency cold plasma nitride carbon steel," *Werkst. Korros.*, vol. 38, p. 417, 1987.

[22] I. Gurappa, "Characterization of different materials for corrosion resistance under simulated body fluid conditions," *Mater. Characterization*, vol. 49, pp. 73-79, 2002.

[23] M. M. Hukovic, A. Kwokal, and J. Piljac, "The influence of niobium and vanadium on passivity of titanium-based implants in physiological solution," *Biomaterials*, vol. 24, pp. 3765-3775, 2003.

[24] G. Rondelli, B. Vicentini, and A. Cigada, "The corrosion behaviour of nickel titanium shape memory alloys," *Corrosion Science*, vol. 30, pp. 805-812, 1990.

[25] M. Niinomi, "Recent research and development in titanium alloys for biomedical applications and healthcare goods," *Science and Technology of Advanced Materials*, vol. 4, pp. 445-454, 2003.

[26] S. Piscanec, L. C. Ciacchi, E. Vesselli, G. Comelli, O. Sbaizero, S. Meriani, and A. De Vita, "Bioactivity of TiN-coated titanium implants," *Acta Material*, vol. 52, pp. 1237-1245, 2004.

[27] K. Matsumoto, N. Tajima, and S. Kuwahara, "Correction of scoliosis with shape-memory alloy," *Nihon Seikeigeka Gakkai Zasshi*, vol. 67, pp. 267-274, 1993.

[28] J. Ryhanen, "Biocompatibility evaluation of nickel-titanium shape memory metal alloy," Dissertation, University of Oulu, 1999.

[29] P. Ypsilantis, M. Politou, D. Mikroulis, M. Pitiakoudis, M. Lambropoulou, C. Tsigalou, V. Didilis, G. Bougioukas, N. Papadopoulos, C. Manolas, and C. Simopoulos, "Organ Toxicity and Mortality in Propofol-Sedated Rabbits Under Prolonged Mechanical Ventilation," *International Anesthesia Research Society*, vol. 105, pp. 155-166, 2007.

DOI: 10.5963/JBAP0501002